Journal of Occupational and Environmental Hygiene

A Novel Algorithm for Determining Contact Area Between a Respirator and a Headform

Zhipeng Lei [a] , James Yang [a] & Ziqing Zhuang [b]

[a] Human-Centric Design Research Lab, Department of Mechanical Engineering , Texas Tech University , Lubbock , Texas

[b] National Institute for Occupational Safety and Health , Pittsburgh , Pennsylvania
Accepted author version posted online: 30 Oct 2013.Published online: 28 Feb 2014.

PLEASE SCROLL DOWN FOR ARTICLE

A Novel Algorithm for Determining Contact Area Between a Respirator and a Headform

Zhipeng Lei,[1] James Yang,[1] and Ziqing Zhuang[2]

[1]Human-Centric Design Research Lab, Department of Mechanical Engineering, Texas Tech University, Lubbock, Texas
[2]National Institute for Occupational Safety and Health, Pittsburgh, Pennsylvania

The contact area, as well as the contact pressure, is created when a respiratory protection device (a respirator or surgical mask) contacts a human face. A computer-based algorithm for determining the contact area between a headform and N95 filtering facepiece respirator (FFR) was proposed. Six N95 FFRs were applied to five sizes of standard headforms (large, medium, small, long/narrow, and short/wide) to simulate respirator donning. After the contact simulation between a headform and an N95 FFR was conducted, a contact area was determined by extracting the intersection surfaces of the headform and the N95 FFR. Using computer-aided design tools, a superimposed contact area and an average contact area, which are non-uniform rational basis spline (NURBS) surfaces, were developed for each headform. Experiments that directly measured dimensions of the contact areas between headform prototypes and N95 FFRs were used to validate the simulation results. Headform sizes influenced all contact area dimensions (P < 0.0001), and N95 FFR sizing systems influenced all contact area dimensions (P < 0.05) except the left and right chin regions. The medium headform produced the largest contact area, while the large and small headforms produced the smallest.

Keywords   headform, respirator, finite element method, contact area

Address correspondence to: James Yang, Human-Centric Design Research Lab, Department of Mechanical Engineering, Texas Tech University, Lubbock, Texas 79409; e-mail: james.yang@ttu.edu

INTRODUCTION

N95 filtering facepiece respirators (FFRs) play an important role in preventing contaminated particles in the environment from entering into the human body. To design an optimal FFR, it is critical to understand the contact mechanism between a respirator and the human face. Due to variation in size and shape, every face has a different contact area with a different respirator. How to easily and efficiently determine the contact area between a respirator and a face is important

for designers. This article presents a simulation-based method to determine the contact area.

The contact area, as well as the contact pressure, is created when a respiratory protection device (a respirator or surgical mask) contacts a human face.[1] When using an N95 FFR or surgical mask, many more aerosol particles leak through the face seal than through the filtering medium. An insufficient contact area contributes to this face seal leakage.[2] Additionally, because a user will feel discomfort if the respirator contacts the eyes and mouth, determining the location of the contact area is critical.[3]

A few papers have studied the method to obtain the contact area between a head and a respiratory protection device. In 1984, Hidson obtained the contact area of a headform and a mask through experimentation.[4] When the mask was placed on the headform, chalk dust was sprayed into the dead space of the mask. The inner boundary curve of the contact area was the boundary of the chalk dust, and the outer boundary curve was the mask's border. In 2010, Dellweg et al. measured the contact area between a mask and a planar surface.[5] The mask was from a non-invasive ventilation widely used in hospitals to provide air to a patient's breathing system. In the experiment, the mask was pushed to contact the surface, leaving color imprints. The mask cushion's color imprints on the surface were the contact area and a planimetric measurement recorded the area size of the color imprints. This method of determining the contact area required that the closed, circular shape of the mask cushion fully contact the planar surface. Since the boundary curve of the N95 FFR was specially designed to fit the shape of the nasal bridge, the contact area of the head/N95 FFR was nonplanar.

Friess determined the respirator seal area using 3D scanning images.[6] A subject's head was captured with and without wearing a respirator. The inner and outer boundary curves of the respirator were drawn. The contact area on the subject's face was created between two sealing outlines with the help of computer-aided design software. Krishnamurthy and Sen proposed an "ideal contact area" for a mask on the human face.[7] According to the mask user's facial geometry, the ideal

contact area of the half face mask was created as a 2D planar curve on the plane that was defined by three facial landmarks (sellion, menton, and pronasale). However, no experimental contact area from existing mask products justified the proposed contact area.

Roberge et al.[8] and Niezgoda et al.[9] proposed a method for determining the N95 FFR face seal area using stereophotogrammetry (STL), a tool for capturing 3D surface information from several 2D photos. First, one obtained 3D surfaces by the STL from two conditions: when the subject donned or did not don the N95 FFR. Second, utilizing computer software (IMInspect of PolyWorks, Innovmetric Software Inc., Quebec City, Quebec, Canada) the two surfaces were aligned for a geometric best fit. Third, the non-intersection areas were removed according to the texture change on overlaid surfaces, and face seal areas were the remaining parts of the 3D surface. This method required the technician to manually manipulate scanned surfaces. The accuracy of results heavily depended on the technician's visual perception.

The health industry has been searching for an accurate representation of the human headform.[10] The National Institute for Occupational Safety and Health (NIOSH) developed a new respirator fit test panel using the principal component analysis method.[11,12] This panel classified subjects into five head size categories: small, short/wide, medium, long/narrow, and large. For demonstrating five categories of head sizes, five standard headforms were created by measuring, selecting, and processing digital headforms from the 3D head scanning database.[13] These five headforms were used to develop five finite element (FE) headforms with high bio-fidelity.[1,14]

The current study presented a simulation-based method to determine contact areas between a human face and an N95 FFR.

METHODOLOGY

As shown in Figure 1, the methodology for determining the contact area between a headform and an N95 FFR contained six steps. First, FE models of a headform and an N95 FFR were constructed. Second, a contact simulation between them was set up. Third, the headform outer surface and the N95 FFR inner surface, which intersect after the contact simulation, were extracted. Fourth, these two surfaces, consisting
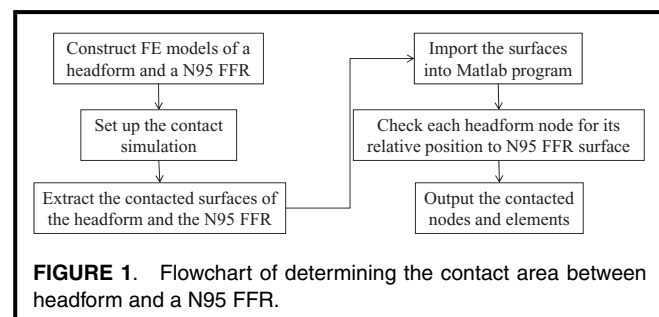

FIGURE 1. Flowchart of determining the contact area between headform and a N95 FFR.

TABLE I. Proper (Fitted) Headform/N95 FFR Combinations, Marked with "X"

| N95 FFR | Headform | | | | |
	Small	Short/ wide	Medium	Long/ narrow	Large
One-size	X	X	X	X	X
Two-size *small/medium*	X	X	X		
Two-size *medium/large*			X	X	X
Three-size *small*	X	X			
Three-size *medium*			X		
Three-size *large*				X	X

Note: X = the proper (fitted) headform/N95 FFR combination considered in this study.

of triangular elements, quadrilateral elements, and nodes, were imported into a Matlab program for further processing. Fifth, each headform node, which was the vertex of a triangular or quadrilateral element, was assessed for its relative position to the N95 FFR surface to determine contact nodes and elements. Finally, contacted nodes and elements from the headform surface were exported.

In Figure 1 Steps 1 and 2 were reported by Lei et al.[1,14] Readers can refer to these references for details. The tested headform/N95 FFR combinations are marked with "X" in Table I.

Contact Area Generation from the Intersection of Surfaces

After contact simulation, the headform surface, referring to the outer surface of the headform, contacted the N95 FFR surface, referring to the inner surface of the N95 FFR filtering medium. The two surfaces intersected; therefore, the contact area could be determined by extracting the intersection area of these two surfaces. An intersection is defined as a set of points common to two or more geometric surfaces. In cases where the headform surface smoothly contacts the N95 FFR surface, the headform points of the contact area have zero distance from the N95 FFR surface. However, the headform and N95 FFR surfaces were discretized into quadrilateral and triangular elements, and conforming contact among the elements in 3D space was nearly impossible. Thus, the definition of the contact area was expanded to indicate a set of points of the headform surface with a very small offset distance (or tolerance) of 0.1 mm from the N95 FFR surface.

The outer surface of the headform and the inner surface of the N95 FFR were extracted from the results of the nonlinear FE contact simulation as a keyword file that stored the information of unstructured surfaces consisting of nodes and triangular or quadrilateral elements, as shown in Figure 2. The format of the keyword file is described in LS-DYNA's Keyword User's Manual.[15] A Matlab program was developed to read the data in the keyword file. The global Cartesian coordinates denoted the nodes of the surfaces, and the indexes of nodes denoted the elements. Three indexes of nodes constituted a triangular element, and four indexes constituted a quadrilateral element. The headform surface was discretized into quadrilateral
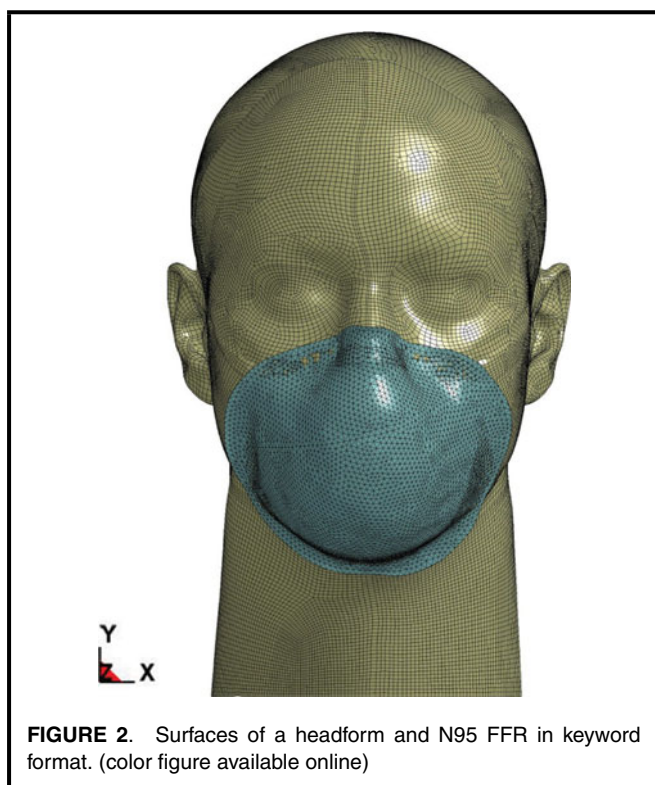
FIGURE 2. Surfaces of a headform and N95 FFR in keyword format. (color figure available online)

elements. A $N \times 3$ matrix (N was the number of headform nodes) and a $M \times 4$ matrix (M was the number of headform elements) mathematically represented the headform surface. Similarly, the N95 FFR surface was expressed as two matrices that collected the data for nodes and elements.

To improve the resolution of the contact area the headform surface with an element size of approximately 2 mm was further refined. Figure 3 explains the procedure of refining headform elements. The lines that connected the middle points in four edges divided the quadrilateral element into four quadrilateral elements. Each newly created quadrilateral element had an element size of approximately 1 mm. Then, the lines that connected the pairs of diagonal nodes split four quadrilateral elements into eight triangular elements. The triangulation transformation was necessary because the stereolithography (STL) format, which can be read by any CAD software (e.g., Autodesk Inventor, San Rafael, Calif.), only saved triangular elements.

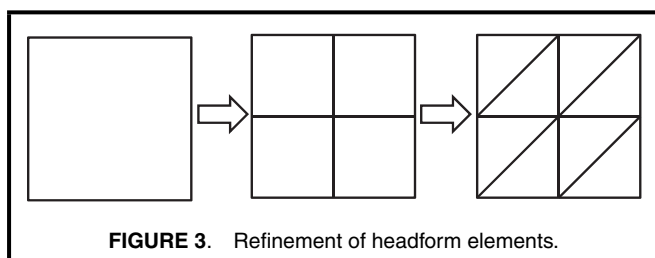Each headform node was checked on whether it contacted the N95 FFR surface. The matrix of headform nodes was traversed, and the distance between each headform node and the N95 FFR surface was calculated. Because the edges of the headform elements were greater than 1 mm, the Matlab program set a relatively small positive tolerance of $\alpha = 0.1$ mm. When the calculated distance of the headform node to the N95 FFR surface was smaller than tolerance α, the headform node was defined as contacting the N95 FFR surface. Headform nodes that contacted the N95 FFR surface were obtained and saved in a separated data set. The triangles of the headform surface that contained the contacted headform nodes were collected and saved in another separate data set. Two data sets of contacted headform nodes and contacted headform elements were used for exporting a STL format file that represented the contact area.

Superimposed Contact Areas and Average Contact Area

The PrePost software (Livermore Software Technology Corporation, Livermore, Calif.) read all headform/N95 FFR contact areas into STL format for further processing. Figure 4a presents the contact area of the medium-size headform/one-size N95 FFR as triangular elements. To represent the 16 contact areas of headform/N95 FFR combinations, 5 superimposed contact areas and 5 average contact areas were created.

For each headform that interacted with its properly fitted N95 FFRs, a superimposed contact area of the headform, as the union of the contact areas of the headform, indicated all areas on the headform surface that contacted any one of the properly fitted N95 FFRs. The superimposed contact area was determined for each headform in four steps. First, different contact areas were imported into the same domain using PrePost software. Second, imported contact areas were merged together as a new surface. Third, the duplicated nodes, which referred to any two nodes that had a distance shorter than a small tolerance, were removed and holes on the surface were filled. The surface and boundary curves were smoothed. Finally, the superimposed contact area was exported in a STL file. Figure 4(b) gives an example of the superimposed contact area from
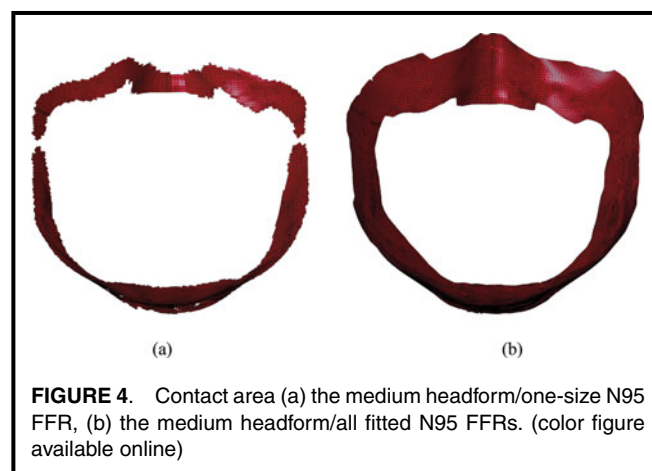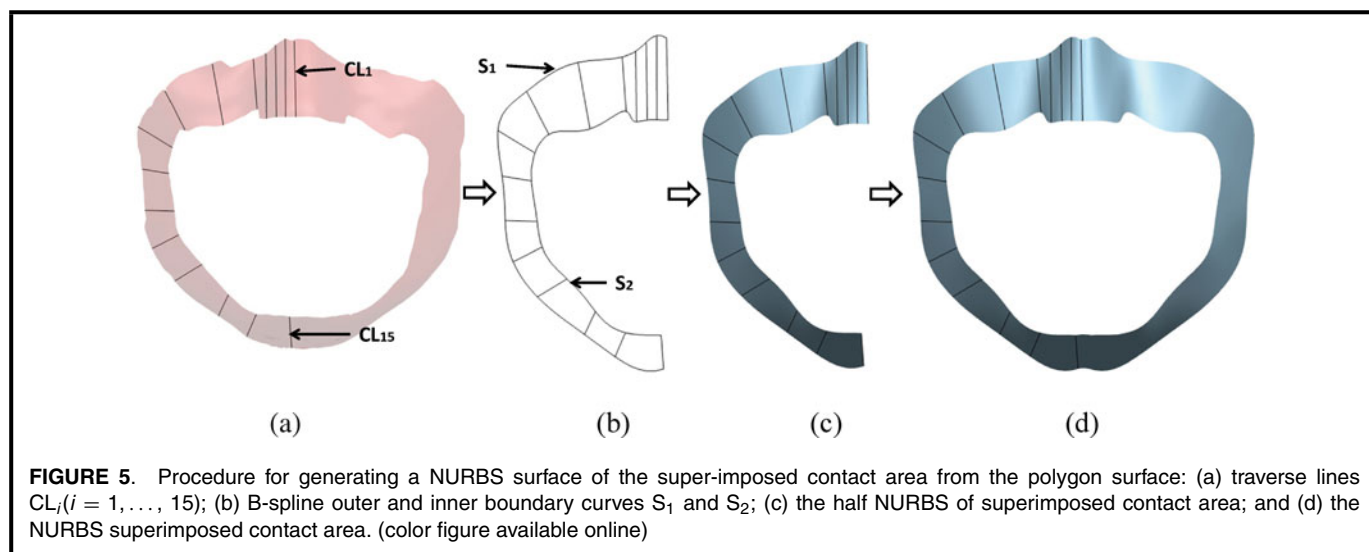

FIGURE 3. Refinement of headform elements.

FIGURE 4. Contact area (a) the medium headform/one-size N95 FFR, (b) the medium headform/all fitted N95 FFRs. (color figure available online)

FIGURE 5. Procedure for generating a NURBS surface of the super-imposed contact area from the polygon surface: (a) traverse lines $CL_i(i = 1, \ldots, 15)$; (b) B-spline outer and inner boundary curves S_1 and S_2; (c) the half NURBS of superimposed contact area; and (d) the NURBS superimposed contact area. (color figure available online)
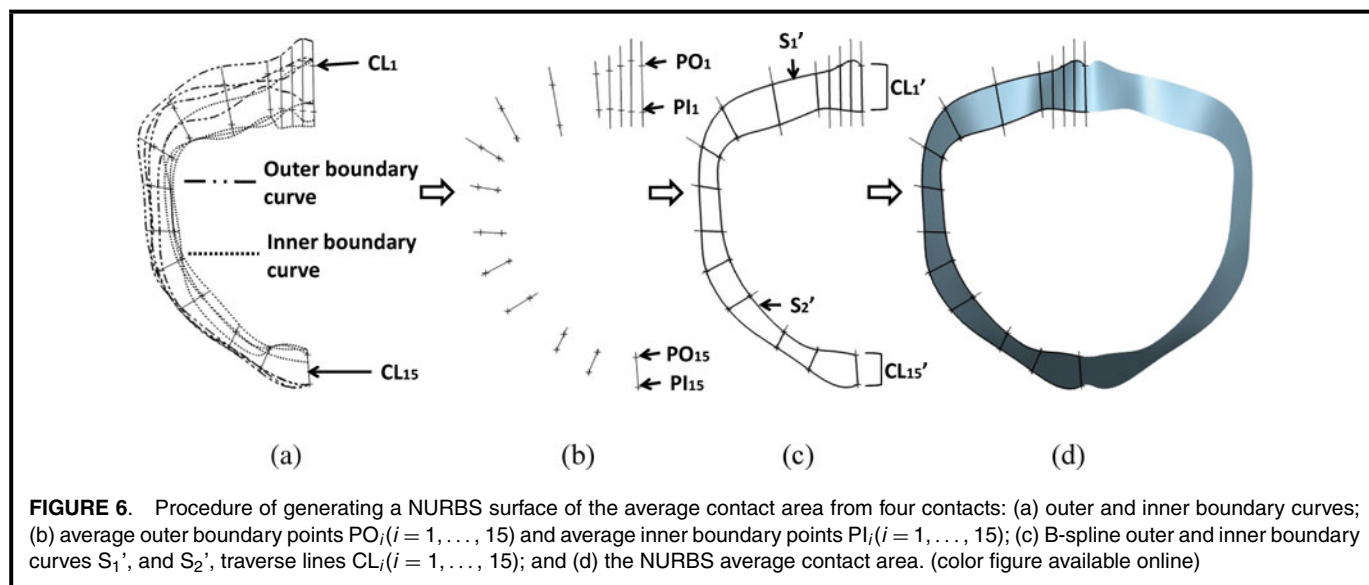
the medium-size headform/N95 FFR combinations. For polygon surfaces, the superimposed contact area in the STL file was converted into the NURBS surface. The NURBS format can be used for analyzing the characteristics of the respirator shape, including its geometrical continuity and control parameters, and for conducting the computer-aided operations of the respirator shape, including cutting, offsetting, and transforming.[3,6]

Figure 6 presents the procedure of generating a NURBS surface based on the superimposed contact area in the format of the polygon surface. The superimposed contact area can be considered as a ring with an inner boundary curve and an outer boundary curve. The NURBS surface of a contact area was assumed to be symmetrical, since both the headforms and the N95 FFRs were designed to be symmetrical, although minor asymmetry existed in all headforms and N95 FFRs. To begin, a half side of the superimposed contact area was generated. Traverse lines $CL_i(i = 1, \ldots, 15)$ which linearly connected the inner boundary curve to the outer boundary

curve, were created. They were drawn on the polygon surface of the superimposed contact area (with red color), as shown in Figure 5a. The locations and directions of traverse lines $CL_i(i = 1, \ldots, 15)$ were carefully selected manually so that they could capture geometrical features of the superimposed contact area. For example, the highly curved region at the nose bridge had a higher density of traverse lines than other regions. Second, the traverse lines' ends at the outer boundary curve were connected to create a B-spline curve S_1. Also, the traverse lines' ends at the inner boundary curve were connected to create another B-spline curve S_2, as shown in Figure 6b.

Third, a NURBS surface that covered the traverse line $CL_i(i = 1, \ldots, 15)$ and B-spline curve S_1 and S_2 was created as a half side of the superimposed contact area, as shown in Figure 5c. Finally, the half side of the NURBS surface was mirrored across the headform's sagittal plane, generating the NURBS superimposed contact area (the blue color surface) in Figure 5d. Since the traverse line $CL_i(i = 1, \ldots, 15)$ and

FIGURE 6. Procedure of generating a NURBS surface of the average contact area from four contacts: (a) outer and inner boundary curves; (b) average outer boundary points $PO_i(i = 1, \ldots, 15)$ and average inner boundary points $PI_i(i = 1, \ldots, 15)$; (c) B-spline outer and inner boundary curves S_1', and S_2', traverse lines $CL_i(i = 1, \ldots, 15)$; and (d) the NURBS average contact area. (color figure available online)

B-spline curve S_1 and S_2 are not exactly located on the headform surface, the proposed method contains a source of error in the calculation of contact area. The source of error can be reduced by using nonlinear traverse lines, each of which is controlled by three or more points instead of two points, and adding more traverse lines.

For each headform that interacts with three respirator systems, an average contact area is the standardized contact area, of which outer and inner boundary curves are created by averaging over all the contact area boundary curves of the headform. The average contact area was determined to represent the ideal contact area between the headform and the three respirator systems. For example, the average contact area of the medium headform was created from the contact areas of medium-size headform/N95 FFR combinations. Since the medium headform was tested on four N95 FFRs, it had four contact areas. Figure 6 describes the procedure of generating a NURBS surface of the average contact area from the four contact areas. Traverse lines $CL_i (i = 1, \ldots, 15)$ which were used in the generation of the superimposed contact area of the medium-size headform, were maintained.

First, the PrePost software processed the four contact areas of medium-size headform/N95 FFR combinations to generate the B-spline curves of the outer and inner boundaries of each of the contact areas. The outer and inner boundary curves were imported into the same coordinate system of the traverse lines $CL_i (i = 1, \ldots, 15)$. Each traverse line had eight intersecting points in which four points were from four outer boundary curves, and four points were from four inner boundary curves. Second, average outer boundary points $PO_i (i = 1, \ldots, 15)$ and average inner boundary points $PI_i (i = 1, \ldots, 15)$ were obtained in traverse lines $CL_i (i = 1, \ldots, 15)$. An average outer boundary point was the average position of four intersection points between four outer boundary curves and the traverse line, and an average inner boundary point was the average position of four intersecting points between four inner boundary curves and the traverse line, as shown in Figure 6b. Third, average outer boundary points $PO_i (i = 1, \ldots, 15)$ formed a B-spline average outer boundary curve S_1', and, similarly, average inner boundary points $PI_i (i = 1, \ldots, 15)$ also formed a B-spline average inner boundary curve S_2', as shown in Figure 6c. New traverse lines $CL_i' (i = 1, \ldots, 15)$ connected average outer boundary points $PO_i (i = 1, \ldots, 15)$ to the average inner boundary points $PI_i (i = 1, \ldots, 15)$. Finally, the NURBS average contact area of a medium-size headform was generated by the method of sweeping the traverse line CL_1' along the boundary curves S_1' and S_2' and mirroring the half side surface, as shown in Figure 6d.

Experimental Measurements and Data Analysis

Experiments were conducted to collect contact area data from headform prototypes and respirators. The contact area of a headform/N95 FFR combination is approximately in the shape of six straight lines that link together to form a closed curve. The vertices of the lines are located at six anatomical sites. The anatomical site of the glabella, the frontal point

in the middle of the two eyebrows and above the nose, was set as a reference point for expressing the relative location of the contact area on the headform. Thus, a total of seven key points, including a) glabella, b) nasal bridge, c) left malar bone, d) right malar bone, e) left gonion, f) right gonion, and g) menton, were defined to describe the shape of the contact area. By connecting these key points, seven dimensions were defined: L_1-upper nose, L_2-left nose, L_3-right nose, L_4-left cheek, L_5-right cheek, L_6-left chin, and L_7-right chin.

Prototypes of the five sizes of headforms, produced by American Precision Prototyping, LLC (Tulsa, OK) with Polypro-Like Accura 25 material, were used in the experiments for validating the simulation results. The Tactilus free form sensor system (Sensor Products, Inc., Madison, N.J.) was incorporated into the experiments. Separate sensors with thin and tactile surfaces made possible measurements on surfaces with complex geometries like a human face. The sensors were placed at desired locations. The hub collected the pressure data and sent the data to the computer via a cable. The Tactilus software collected and stored the results. A vernier caliper was used to measure the linear distance.

The N95 FFRs were placed on the headform prototypes. As shown in Figure 7a, pressure sensors determined seven anatomical key points A–G in the contact area of a headform/N95 FFR combination. Then the vernier caliper measured the seven dimensions $L_i (i = 1, \ldots, 7)$ of the contact area. In one headform/N95 FFR combination, each dimension of the contact area was measured three times by using three experimental N95 FFRs to consider the variation between different experimental N95 FFRs that were the same type and brand. In addition, the three repeated measurements were conducted on different days.

As shown in Figure 7b, the PrePost software determined the seven anatomical key points A–G and the seven dimensions $L_i (i = 1, \ldots, 7)$ for the computer model. The PrePost software was used to calculate the distance between two anatomical key points to determine the contact area dimensions. In our study, we determined each dimension of the contact area three times to consider the positional errors of anatomical key points.

Each contact area had an outer boundary curve and an inner boundary curve. It was experimentally too difficult to measure the contact area dimensions at inner boundary curves. For comparison of experimental and simulation results, only dimensions at the contact areas' outer boundary curves could be used. The contact area dimensions, if not specified explicitly, were all measured at the outer boundary curves of contact areas.

Table II gives a summary of the data sampling in this study. The mean value and standard deviation (SD) were calculated from the three-time repeated experimental measures for a contact area dimension in a headform/N95 FFR combination. To compare the experimental results to the simulation results, a linear regression analysis was performed between experimental and simulation mean values.

A one-way analysis of variance (ANOVA) was used to test whether values of a contact area dimension, obtained from five different headform sizes, were significantly different from
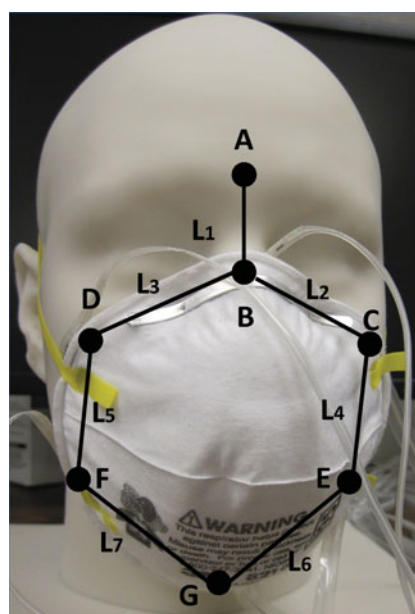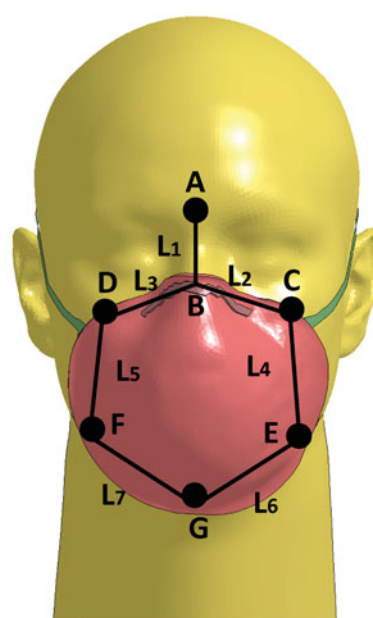
FIGURE 7. (a) Experimental measurements of contact area dimensions of a headform/N95 FFR combination; (b) computer-based determinations of contact area dimensions of a headform/N95 FFR combination (A: glabella, B: nasal bridge, C: left malar bone, D: right malar bone, E: left gonion, F: right gonion, and G: menton, L_1: upper nose, L_2: left nose, L_3: right nose, L_4: left cheek, L_5: right cheek, L_6: left chin, L_7: right chin). (color figure available online)

one another. The upper nose was used as an example. The medium-size headform had four contact areas from four different respirators. For each contact area, the length of the upper nose was experimentally measured and determined through simulation three times. The values of the upper nose length were divided into five groups according to headform size. The one-way ANOVA evaluated the differences among these five groups of values. If the P-value was below 0.05, the different headform sizes impacted the upper nose length.

Additionally, ANOVA was used to test whether values of a contact area dimension from three different sizing systems of N95 FFRs (one-size, two-size, and three-size) were significantly different from one another.

RESULTS

Table III presents experimental means and SDs of contact area dimensions in headform/one-size N95 FFR combina-

tions. Table IV presents simulation means and SDs of contact area dimensions in headform/one-size N95 FFR combinations. Eighty percent (28 out of 35) of differences between experimental and simulation mean values are below 2 mm. Similarly, one can obtain contact area dimensions for headform/two-size N95 FFR combinations and headform/three-size N95

TABLE II. A Summary of the Data Sampling

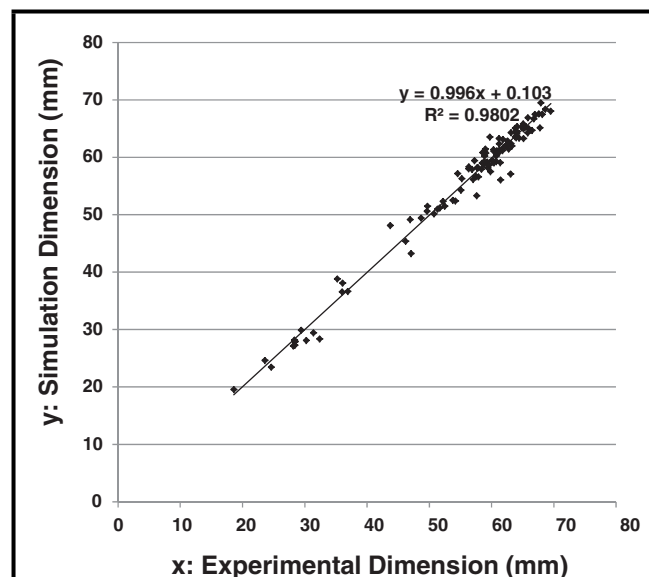|	
Sizes of headforms	5
Sizing systems of N95 FFRs	3
Types of results	2 (experiment and simulation)
Total headform/N95 FFR combinations	16
Contact area dimensions	7
Replicates	3

FIGURE 8. Comparison of contact area dimensions of headform/N95 FFR combinations.

TABLE III. Experimental Means and SDs of Contact Area Dimensions in Headform/One-Size N95 FFR Combinations (units: mm)

Headform	Mean (SD)						
	Upper nose	Left nose	Right nose	Left cheek	Right cheek	Left chin	Right chin
Small	18.61 (1.17)	59.41 (0.77)	59.68 (0.75)	61.83 (0.35)	59.74 (0.38)	61.45 (0.40)	63.08 (0.34)
Short/wide	29.43 (0.34)	64.01 (0.38)	64.87 (0.51)	57.68 (0.72)	58.49 (0.37)	51.69 (1.33)	51.33 (0.47)
Medium	36.08 (0.76)	58.88 (0.20)	60.37 (0.92)	61.21 (0.44)	62.59 (0.65)	57.61 (0.67)	57.84 (0.47)
Long/narrow	36.02 (0.46)	62.33 (0.20)	61.25 (0.22)	62.04 (0.65)	62.76 (0.67)	56.36 (0.55)	57.07 (1.16)
Large	35.25 (0.50)	64.06 (0.23)	63.81 (0.37)	65.86 (0.31)	65.50 (0.63)	52.20 (0.29)	52.49 (0.06)

FFR combinations. In Figure 8 the horizontal axis indicates the dimension of the headform/N95 FFR contact area from experimental data. The vertical axis indicates the dimension of the headform/N95 FFR contact area from simulation results and provides a linear regression analysis on experimental and simulation results. A R^2 value of 0.9802 indicates that the computational results have a strong correlation with experimental results. The maximum error of the simulation results is 6.02 mm, and 82% of the errors are below 2 mm.

In Table V, the single factor ANOVA tests the difference in the values of a contact area dimension among different headform sizes as well as tests the difference in the values of the contact area dimension among different N95 FFR sizing systems ($\alpha = 0.05$). Seven contact area dimensions were examined individually. The headform sizes influenced all contact area dimensions ($P < 0.0001$); N95 FFR sizing systems influenced all contact area dimensions ($P < 0.05$) except for the left and right chin.

Figure 9 presents the superimposed contact areas of headform/N95 FFR combinations for the five sizes of headforms: (a) small, (b) short/wide, (c) medium, (d) long/narrow, and (e) large. Figure 10 presents average contact areas of headform/N95 FFR combinations for the five sizes of headforms. Contact area dimensions at their outer and inner boundaries were determined three times in simulation. Because the outer and inner boundaries were created as symmetric curves, seven dimensions were reduced to four dimensions: the upper nose, left/right nose, left/right cheek, and left/right chin.

Table VI provides mean values and SDs of contact area dimensions for five superimposed contact areas at two bound-

aries. Table VII provides mean values and SDs of contact area dimensions for five average contact areas at two boundaries. Table VIII provides sizes of superimposed contact areas and average contact areas among the five sizes of headforms. Superimposed contact areas ranged from 6451.79 to 9285.24 mm^2, and average contact areas ranged from 4115.25 to 6135.68 mm^2. The medium headform had the largest contact area size, while the large and small headforms had the smallest contact area sizes.

DISCUSSION

In this study, a computer-based method was described for determining contact areas of headform/N95 FFR combinations. Experiments were primarily used for validating simulation results. The experimental method had two limitations. One limitation was that the experiments could only perform 2D measurements of two-point distances. The simulation results provided 3D positions of any points in the contact areas.

The second limitation was that it was difficult to measure the inner boundaries of contact areas. The inner boundaries were covered by the N95 FFR filtering medium. An N95 FFR contact area had a narrow width between the outer boundary curve and the inner boundary curve. Parts of the contact area had widths lower than 1 cm, while the size of the pressure sensor was 0.8×0.8 cm^2. The position of the inner boundary could not be accurately located by the pressure sensor. Thus, the computer-based approach was preferable to the experimental approach for determining headform/N95 FFR contact areas.

TABLE IV. Simulation Means and SDs of Contact Area Dimensions in Headform/One-Size N95 FFR Combinations (units: mm)

| Headform	Mean (SD)						
	Upper nose	Left nose	Right nose	Left cheek	Right cheek	Left chin	Right chin
Small	19.54 (1.05)	58.15 (1.71)	58.65 (1.60)	63.11 (0.91)	63.53 (0.83)	56.05 (0.22)	57.06 (0.36)
Short/wide	29.87 (0.37)	64.57 (1.05)	65.25 (0.57)	58.19 (1.80)	58.98 (0.49)	51.17 (0.64)	50.98 (0.41)
Medium	38.09 (0.46)	61.04 (0.40)	61.04 (0.73)	63.26 (0.45)	62.84 (0.72)	53.29 (0.37)	58.16 (0.28)
Long/narrow	36.55 (0.54)	62.07 (0.22)	62.32 (1.48)	61.77 (0.30)	61.41 (0.76)	58.34 (0.86)	56.13 (0.49)
Large	38.80 (0.95)	64.11 (0.17)	63.57 (0.21)	66.87 (1.22)	65.27 (0.86)	52.32 (0.64)	51.45 (1.25)
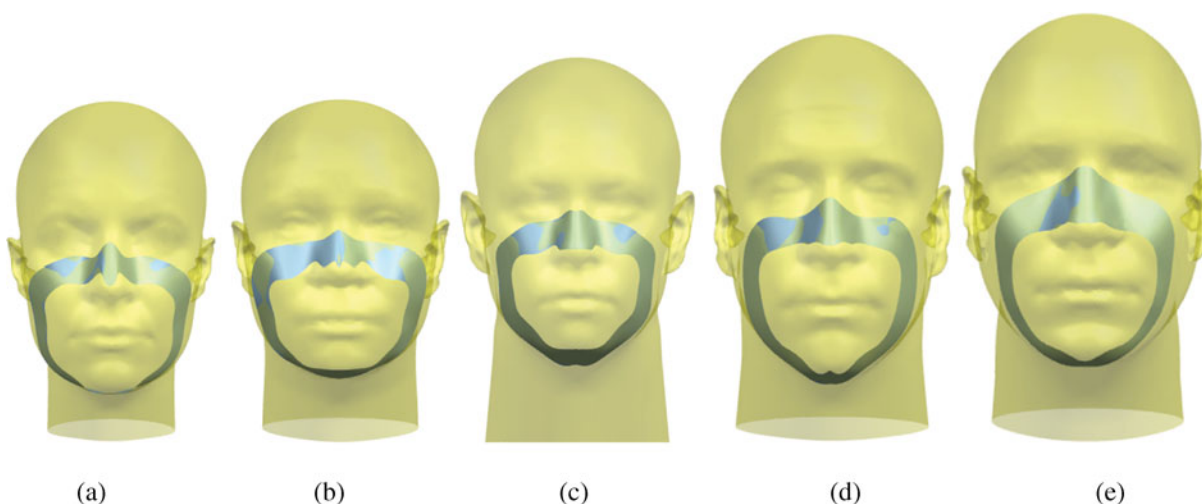
FIGURE 9. Superimposed contact areas of headform/N95 FFR combinations for the five sizes of headforms: (a) small; (b) short/wide; (c) medium; (d) long/narrow; and (e) large. (color figure available online)

Joe et al. proposed a computer-based approach to measure facial parameters.[16] A 3D laser scanner captured the head surfaces of subjects. Reverse engineering software processed the scanned data and determined anthropometric dimensions. When compared with the traditional method, this computer-based method produced large errors (the maximum difference was 12.8 mm). The errors came from two sources: movement of the subject's head during scanning and low-quality processing for the 3D scanned heads. The computer-based approach to determine contact area dimensions of headform/N95 FFR combinations presented in this article produced smaller errors (the maximum difference from experimental results was 6.02 mm and 82% of them were within 2 mm). During experiments, headform prototypes, unlike human subjects, could be easily maintained in a static state. The digital headform models were good quality.[13] Each of five headform prototypes from the experiments had exactly the same surface geometry as the matching digital headform developed by NIOSH. Thus, the method proposed in this article overcame the disadvantages of the method of Joe et al.[16]

NIOSH found the correlation between the subject's face size and respirator fit.[17] This study indicated that headform sizes influenced all contact area dimensions ($P < 0.0001$) and that N95 FFR sizing systems influenced all contact area dimensions ($P < 0.05$) except the left and right chin regions. Only six N95 FFRs were used in this study. It is possible that, when other brands of N95 FFRs are considered in contact area studies, all contact area dimensions would be influenced.
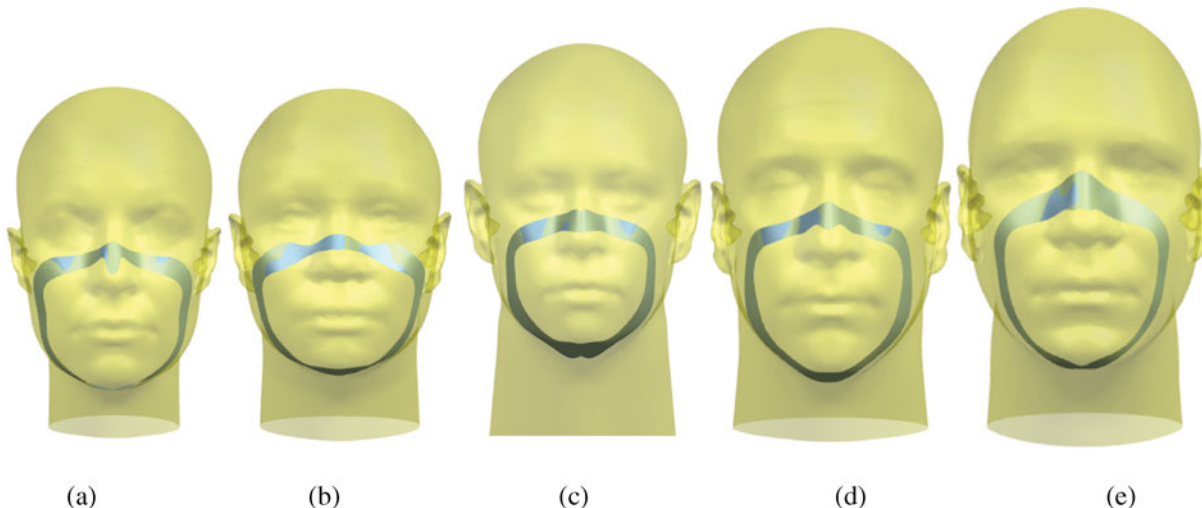

FIGURE 10. Average contact areas of headform/N95 FFR combinations for the five sizes of headforms: (a) small; (b) short/wide; (c) medium; (d) long/narrow; and (e) large. (color figure available online)

TABLE V. Results of the Single Factor ANOVA That Tests the Difference in the Values of a Contact Area Dimension among Different Headform Sizes and Tests the Difference in the Values of the Contact Area Dimension among Different N95 FFR Sizing Systems ($\alpha = 0.05$)

	P-value	
Dimension	**Headform**	**N95 FFR sizing system**
Upper nose	<0.0001	= 0.0148
Left nose	<0.0001	= 0.0003
Right nose	<0.0001	= 0.0002
Left cheek	<0.0001	= 0.0031
Right cheek	<0.0001	< 0.0007
Left chin	<0.0001	= 0.4295
Right chin	<0.0001	= 0.2458

The contact area between a headform and a respiratory protection device can be used in redesigning the shape of a respiratory protection device to improve fit and comfort.[3,7] In this study, a superimposed contact area and an average contact area of headform/N95 FFR combinations were developed for each of the five sizes of headforms. The superimposed contact area was the union of the contact areas that were generated from the combinations of the headform and three sizing systems of N95 FFRs, while the average contact area was the mean of the contact areas. One limitation in this study is that only six N95 FFR models were used. Future studies will apply the method developed in this article to an increased number of N95 FFR models to determine the superimposed contact area, which provides the area of the headform that could be the N95 FFR contact area, and the average contact area, which represents where a best-fitted N95 FFR should ideally contact.

Values of superimposed contact areas were from 6451.79 to 9285.24 mm^2, and values of average contact areas were from 4115.25 to 6135.68 mm^2. From the study of Niezgoda et al.,[9] the measured contact areas of subject/N95 FFR combinations were in the range of 5950–7290 mm^2, an approximately 1500 mm^2 difference from the average contact area range calculated in our study. Different head sizes between Niezgoda's human subject study and headform sizes in the current study contributed to different values of contact area sizes. Also, different N95 FFRs were used in these two studies.

Unlike real human heads with deformable skin, the headform prototypes used in this study could not deform. Further investigation will experimentally measure respirator contact areas on real subjects. Meanwhile, FE head models will be built from scanning the subjects' heads, and respirator contact areas will be determined using the proposed simulation method. For real subjects, the differences between the experimental and simulation contact areas will be examined.

TABLE VI. Simulation Means and SDs of Contact Area Dimensions in Five Super-Imposed Contact Areas at Outer and Inner Boundaries (units: mm)

	Outer boundary-Mean (SD)				Inner boundary-Mean (SD)			
Headform	**Upper nose**	**Left/right nose**	**Left/right cheek**	**Left/right chin**	**Upper nose**	**Left/right nose**	**Left/right cheek**	**Left/right chin**
Small	18.07 (0.80)	67.41 (0.78)	63.18 (0.87)	50.76 (0.82)	51.80 (1.42)	59.71 (0.44)	47.22 (0.60)	45.53 (1.03)
Short/wide	27.59 (0.15)	63.42 (0.78)	65.75 (0.77)	57.62 (0.65)	55.56 (0.59)	55.10 (0.51)	44.76 (1.10)	46.41 (0.69)
Medium	23.63 (0.55)	67.15 (0.75)	60.69 (0.60)	38.67 (0.58)	55.48 (0.73)	58.55 (0.17)	38.67 (0.58)	54.28 (0.59)
Long/narrow	28.07 (1.24)	60.71 (0.07)	67.51 (0.52)	58.30 (0.31)	60.71 (0.07)	59.70 (0.51)	51.48 (1.21)	45.78 (0.95)
Large	19.68 (0.59)	63.14 (0.46)	68.84 (0.96)	58.33 (0.76)	59.37 (0.55)	56.15 (0.45)	49.81 (1.17)	46.70 (0.74)

TABLE VII. Simulation Means and SDs of Contact Area Dimensions in Five Average Contact Areas at Outer and Inner Boundaries (units: mm)

	Outer boundary-Mean (SD)				Inner boundary-Mean (SD)			
Headform	**Upper nose**	**Left/right nose**	**Left/right cheek**	**Left/right chin**	**Upper nose**	**Left/right nose**	**Left/right cheek**	**Left/right chin**
Small	23.20 (0.26)	60.16 (1.09)	63.43 (1.27)	49.15 (0.41)	44.90 (1.21)	57.71 (0.50)	51.20 (1.15)	49.35 (0.56)
Short/wide	28.75 (1.17)	64.12 (0.82)	58.47 (0.65)	51.98 (0.78)	37.18 (0.81)	57.51 (0.95)	43.58 (0.57)	49.35 (0.46)
Medium	29.79 (0.96)	60.19 (1.27)	64.01 (0.74)	57.25 (1.01)	51.30 (1.06)	58.50 (0.24)	50.26 (1.09)	45.55 (0.50)
Long/narrow	30.83 (0.02)	61.24 (0.85)	65.17 (0.46)	57.38 (0.61)	51.72 (0.54)	59.33 (0.80)	53.16 (1.07)	49.04 (0.46)
Large	27.93 (0.66)	66.07 (0.29)	65.21 (0.56)	54.03 (0.67)	52.99 (0.49)	58.58 (0.45)	56.74 (0.60)	46.25 (0.90)

TABLE VIII. Sizes of Super-Imposed Contact Areas and Average Contact Areas among the Five Sizes of Headforms

Headform	Size of contact area (mm^2)	
	Super-imposed	Average
Small	6451.79	4115.25
Short/wide	8500.95	5019.25
Medium	9285.24	6135.68
Long/narrow	8989.99	5614.12
Large	7842.18	4730.79

Since this study only determined contact areas of N95 FFRs on static headforms, the influence of head movements on contact areas has not been evaluated. Additionally, whether various computational parameters influence contact areas has not been studied. These parameters defined in LS-DYNA software include the mechanical properties of human tissues, mesh sizes of FE models, the contact friction coefficient between a headform and an N95 FFR, and strap forces. In addition, further investigation will study the correlation between the contact area and respirator fit.

CONCLUSION

This study proposed a novel algorithm for determining the contact area between a headform and an N95 FFR. This algorithm used the FE method to simulate the contact process, then generated the contact area from the intersection of the headform and the N95 FFR surfaces. The algorithm obtained a total of 16 contact areas for different proper combinations between N95 FFRs and headforms. Experiments that directly measured dimensions of contact areas between headform prototypes and N95 FFRs validated these 16 contact areas. To study the factors that influenced contact area dimensions, statistical tests were set up and found that headform sizes affected all contact area dimensions ($P < 0.0001$), and that N95 FFR sizing systems affected all contact area dimensions ($P < 0.05$) except the left and right chin regions. The medium headform produced the largest contact area, while the large and small headforms produced the smallest contact areas.

Five superimposed contact areas and five average contact areas of headform/N95 FFR combinations can be used for improving the shapes of six types of N95 FFRs that were used in this study. To fit a headform, an improved N95 FFR should have a shape that is located within the headform's superimposed contact area and best covers the headform's average contact areas. Once more types of N95 FFRs are used for generating superimposed contact area and average contact area, the determined contact areas can be used in the future study of the N95 FFR customized design that is to fit individual people or target proportions of the population. Further, the method to determine contact area can be

used for designing N95 FFR straps. Based on the equation Force = Pressure × Area, multiplying a contact area size by a contact pressure value produces the force that indicates the target magnitude of the force from the straps of the N95 FFR. Future studies will focus on involving more N95 FFR brands in contact simulations, examining the influence of head movements on contact areas, and conducting a sensitivity analysis of computational parameters.

DISCLAIMER

The findings and conclusions in this article are those of the authors and do not necessarily represent the views of the National Institute for Occupational Safety and Health.

REFERENCES

1. **Lei, Z., J. Yang, and Z. Zhuang:** Contact pressure of N95 filtering facepiece respirators using finite element method. *Computer Aided Design Appl. 7*(6):847–861 (2010).
2. **Grinshpun, S. A., H. Haruta, R. M. Eninger, T. Reponen, R. T. McKay, and S.-A. Lee:** Performance of an N95 filtering facepiece particulate respirator and a surgical mask during human breathing: Two pathways for particle penetration. *J. Occup. Environ. Hyg. 6*(10):593–603 (2009).
3. **Han, D., J. Rhi, and J. Lee:** Development of prototypes of half-mask facepieces for Koreans using the 3D digitizing design method: A pilot study. *Ann. Occup. Hyg. 48*(8):707–714 (2004).
4. **Hidson, D. J.:** *Computer-aided Design of a Respirator Facepiece Model.* Defense Research Establishment, Ottawa, Canada, 1984.
5. **Dellweg, D., D. Hochrainer, M. Klauke, J. Kerl, G. Eiger, and D. Kohler:** Determinants of skin contact pressure formation during non-invasive ventilation. *J. Biomech. 43*(4):652–657 (2010).
6. **National Institute For Occupational Safety and Health:** *Analysis of 3d Data for the Improvement of Respirator Seals,* by M. Friess (Final Report). Anthrotech, Yellow Springs, Ohio, 2004.
7. **Krishnamurthy, H., and D. Sen:** Deriving statistical fit contours and shape of an aerosol mask from 3D head scans. *Int. J. Human Factors Model. Simul. 2*(4):293–313 (2011).
8. **Roberge, R., G. Niezgoda, and S. Benson:** Analysis of forces generated by N95 filtering facepiece respirator tethering devices: A pilot study. *J. Occup. Environ. Hyg. 9*(8):517–523 (2012).
9. **Niezgoda, G., J. Kim, R. Roberge, and S. Benson:** Flat fold and cup-shaped N95 filtering facepiece respirator face seal area and pressure determinations: a stereophotogrammetry study. *J. Occup. Environ. Hyg. 10*(8):419–424 (2013).
10. **Luximon, Y., R. Ball, and L. Justice:** The 3D Chinese head and face modeling. *Computer-Aided Design 44*(1):40–47 (2012).
11. **Zhuang, Z., and B. Bradtmiller:** Head-and-face anthropometric survey of U.S. respirator users. *J. Occup. Environ. Hyg. 2*:567–576 (2005).
12. **Zhuang, Z., B. Bradtmiller, and R.E. Shaffer:** New respirator fit test panels representing the current U.S. civilian work force. *J. Occup. Environ. Hyg. 4*(9):647–659 (2007).
13. **Zhuang, Z., S. Benson, and D. Viscusi:** Digital 3-D headforms with facial features representative of the current U.S. workforce. *Ergonomics 53*(5):661–671 (2010).

14. **Lei, Z., J. Yang, and Z. Zhuang:** Headform and N95 filtering facepiece respirator interaction: Contact pressure simulation and validation. *J. Occup. Environ. Hyg. 9(1)*:46–58 (2011).

15. **Livermore Software Technology Corporation (LSTC):** *LS-DYNA Keyword User's Manual.* Volume I, Version 971. Livermore, CA: Livermore Software Corporation, 2007.

16. **Joe, P.S., Y. Ito, A.M. Shih, R.K. Oestenstad, and C.T. Lungu:** Comparison of a novel surface laser scanning anthropometric technique to traditional methods for facial parameter measurements. *J. Occup. Environ. Hyg. 9(2)*:81–88 (2011).

17. **Zhuang, Z., D. Groce, H.W. Ahlers, et al.:** Correlation between respirator fit and respirator fit test panel cells by respirator size. *J. Occup. Environ. Hyg. 5(10)*:617–628 (2008).